Contents lists available at ScienceDirect

Physics and Imaging in Radiation Oncology

Technical Note

A compact scintillator-based detector with collimator and shielding for dose monitoring in boron neutron capture therapy

Anita Caracciolo [a,b], Tommaso Ferri [a,b], Giacomo Borghi [a,b], Marco Carminati [a,b], Nicoletta Protti [c,d], Saverio Altieri [c,d], Carlo Fiorini [a,b,*]

[a] Dipartimento di Elettronica, Informazione and Bioingegneria, Politecnico di Milano, Milano 20133, Italy
[b] Istituto Nazionale di Fisica Nucleare (INFN), Sezione di Milano, Milano 20133, Italy
[c] Dipartimento di Fisica, Università di Pavia, Pavia 27100, Italy
[d] Istituto Nazionale di Fisica Nucleare (INFN), Sezione di Pavia, Pavia 27100, Italy

ARTICLE INFO

ABSTRACT

Boron neutron capture therapy exploits $^{10}B(n,\alpha)^7Li$ reactions for targeted tumor destruction. In this work, we aimed at developing a dose monitoring system based on the detection of 478 keV gamma rays emitted by the reactions, which is very challenging due to the severe background present. We investigated a compact gamma-ray detector with a pinhole collimator and shielding housing. Experimental nuclear reactor measurements involved varying boron concentrations and artificial shifts of the sources. The system successfully resolved the 478 keV photopeak and detected 1 cm lateral displacements, confirming its suitability for precise boron dose monitoring.

1. Introduction

Boron Neutron Capture Therapy (BNCT) is a targeted radiotherapy technique in which patients are administered boron-10 compounds capable of accumulating preferentially within cancer cells and then are irradiated with epithermal neutron. $^{10}B(n,\alpha)^7Li$ reactions locally damage cancer cells and spare healthy tissues, providing a treatment tailored to tumor shape and location [1]. Given the correlation between the dose and the boron distribution, BNCT relies on optimizing boron-drug uptake in tumor cells while minimizing normal tissue uptake (ideally 20 to 50 μg of ^{10}B with a 3:1 tumor-to-normal tissue ratio [2]). Consequently, monitoring boron concentration within the body is of crucial importance. Real-time verification is preferred over indirect methods like Inductively Coupled Plasma [3] and Positron Emission Tomography [4] due to the dynamic nature of boron distribution. To this aim, different systems were proposed to image the spatial distribution of boron-neutron capture reactions exploiting the 478 keV prompt gamma rays emitted in 94% of them, based either on Single Photon Emission Tomography (SPECT) technique [5–10] or on Compton cameras [11,12]. However, due to the low signal intensity and high background radiation, the selection of detector materials and configurations resulted constrained and no existing device proved to be suitable for clinical use yet. This study proposes a SPECT system based on a gamma-ray detector

built with a monolithic LaBr$_3$ scintillator, an array of silicon photo-multipliers, custom electronics and a pinhole collimator and aims at demonstrating its capability to detect and image boron-neutron capture reactions.

2. Material and methods

Traditional SPECT systems detect low-energy gamma rays emitted by radioisotopes administered to the patient, e.g. Tc-99m emitting photons at 140 keV. A BNCT-SPECT system must be designed to identify higher energy gamma rays, specifically those at 478 keV emitted by the boron compounds in tumor cells. This acquisition has to occur during treatment, requiring a detector with high detection efficiency to discern the low boron signal over the large background. Additionally, good energy resolution is required to separate the 478 keV peak from the adjacent peak at 511 keV due to annihilation photons. Regarding the spatial accuracy, a 1 cm resolution is currently considered acceptable for an effective treatment verification [5,6].

2.1. Gamma ray detector

The proposed gamma-ray detector, visible in the inset of Fig. 1, was based on a co-doped lanthanum bromide LaBr$_3$(Ce + Sr) scintillator

---

* Corresponding author.

crystal produced by Saint Gobain crystals, read by a matrix of 8 × 8 NUV-HD silicon photomultipliers (SiPMs), fabricated by Fondazione Bruno Kessler [13]. The crystal had a surface of $5 \times 5\,cm^2$, matching the dimension of the SiPM matrix, and a thickness of 2 cm that allowed a detection efficiency of 60% at 478 keV. It exhibited excellent energy resolution (<3% at 662 keV), high scintillation yield (73 ph/keV) and quick output pulse (decay time of 25 ns). The outputs of the SiPMs were processed by very compact readout electronics (encumbrance of $6.2 \times 6.2 \times 3\,cm^3$), including four 16-channels custom Application-Specific Integrated Circuit (ASIC) that enabled charge-to-voltage conversion and programmable gain [14]. The ASICs output voltages were then sequentially digitized by four 13-bit analog-to-digital converter at 5 Msps. Both the data acquisition of the digitized value and the ASICs' programming were controlled by a Spartan Field-Programmable Gate Array (FPGA). The ASIC dead time was around 10 μs. Previous detector prototypes successfully identified the 478 keV photopeak during neutron irradiation [15,16]. The current version introduced a square, thinner scintillator crystal and compact readout electronics with direct FPGA integration onto the module. The thinner crystal, combined with the collimator, enabled imaging measurements, while the reduced detector dimensions enhanced space efficiency in view of the final SPECT apparatus.

2.2. Pinhole collimator

The collimator was designed to efficiently attenuate the 478 keV gamma rays and the high-energy background gamma rays (e.g. the 2200 keV from hydrogen neutron captures) enabling a spatial resolution lower than 1 cm [5]. Small size, low weight and low neutron activation of the material were other important parameters. Design optimization was performed by means of ANTS2 simulations (Advanced Neutron Transport Simulation) [17], opting for a lead pinhole collimator, with a thickness of 10 cm. The aperture angle was set to 9.25°, in order to fit a Field Of View (FOV) of $5 \times 5\,cm^2$ on the patient, equal to the crystal surface, when positioned at a distance of 25 cm from both the patient

and the detector (for a total distance patient-detector of 60 cm including also the collimator thickness). The collimator featured a spatial resolution of 8 mm and a geometric efficiency of 3.84×10^{-6} at 478 keV in simulations.

2.3. Shielding housing

During BNCT treatments, significant radiation background made of neutrons and photons of different origin is expected. The primary purpose of the shielding housing is to prevent neutron activation of the detector. Extensive investigations were conducted using both experimental measurements and FLUKA simulations [18] to study the effects of thermal neutrons on the detector. These investigations highlighted a significant background peak at (and in the vicinity of) 478 keV, mainly due to the boron content of the printed circuit boards' FR-4 material, but also due to neutron activation of the scintillator crystal. 0.5 mm-thick cadmium sheets were chosen as shielding material because of the high cross section for thermal neutrons (19,852 b for ^{113}Cd), relative affordability and ease of handling. Two 4 mm-thick lead foils were interposed on the lateral sides, between the cadmium and the detector, to reduce the cadmium-neutron-capture gamma rays at 558 keV and 651 keV.

2.4. Experimental measurements

Experimental measurements to characterize the detector module, including the collimator and the shielding, were carried out inside the Prompt Gamma Neutron Activation Analysis facility of the TRIGA Mark II research nuclear reactor of Pavia University [19]. The detector, covered by its shielding housing, was positioned at a distance of 40 cm from the irradiation target, due to irradiation site constraints. This resulted in a limited FOV of the collimator, that was placed between the two, of around 3.3 cm. The target, a rectangular sample ($4.1 \times 0.3 \times 1.6\,cm^3$), was exposed to a thermal neutron flux of approximately $2 \times 10^6\,n/cm^2/s$.

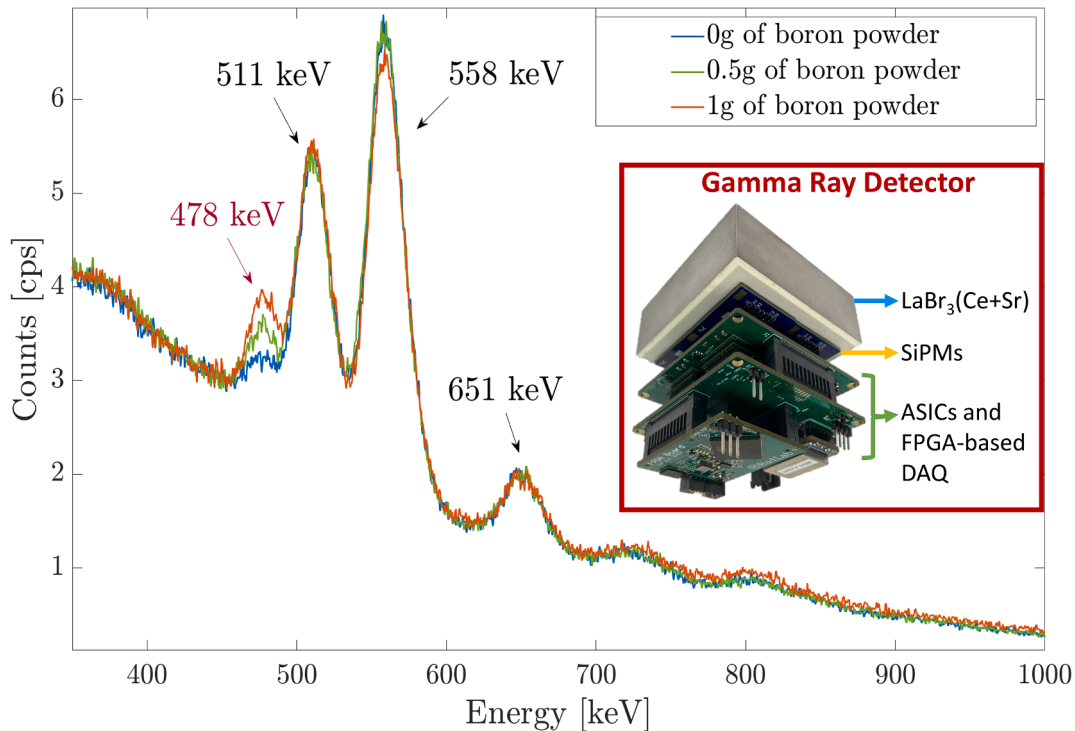First, to assess the linear response of the detector, measurements

Fig. 1. Spectra acquired with the gamma ray detector visible in the inset, based on a LaBr$_3$(Ce + Sr) crystal coupled to a matrix of 8 × 8 SiPMs. Vials loaded with different boron quantities (0 g, 0.5 g, 1 g) were irradiated. The peak at 478 keV increases with the boron quantity. The other visible peaks are due to annihilation photons (511 keV) and cadmium neutron capture reactions (558 keV and 651 keV).

with vials containing different amounts of boron were performed. Three vials were used: one with no boron as background reference, and the other two loaded with 0.5 g and 1 g of amorphous boron powder (20% of boron-10), respectively. For each vial, two measurements of 5 min each were acquired. Matlab was employed to analyze the data and to determine the photopeak characteristics at 478 keV. This process included fitting the spectrum within the range of 440 keV to 540 keV using a custom function, consisting of a straight line for the background and two gaussian functions for the photopeaks at 478 keV and 511 keV. The width and height parameters of the 478 keV peak were then used to calculate the peak area. Finally, a correction factor that accounted for the system dead time (τ) was required given the high counting rate at the detector on the order of tens of thousands of cps. This factor was estimated for each measurement as the ratio between the measured count rate (m) and the true count rate (n$=\frac{m}{1-m\tau}$) [20].

Subsequent measurements were performed to evaluate the imaging capabilities of the system. The vial filled with 1 g of boron was shifted 1 cm away from its initial position and the goal was to track this shift by reconstructing the interaction position of the gamma rays at 478 keV on the monolithic crystal. After conducting a comparative study on machine learning algorithms, an Artificial Neural Network (ANN) was chosen for this task due to its great performance and low computation costs. The ANN featured 64 input neurons for the 64 SiPM signals, one hidden layer with 50 neurons, and an output layer with 2 neurons for the x and y position coordinates. The dataset employed for training (60%), validation (30%), and testing (10%) was obtained through a combination of experimental measurements using a 1 mm collimated cesium source, and simulations conducted with ANTS2. The reconstructed images underwent image processing, including linear calibration, background subtraction (e.g., measurement at 0 g) and normalization of pixel intensities.

3. Results

3.1. Spectroscopic results

The acquired spectra, visible in Fig. 1, showed a distinct BNCT photopeak at 478 keV, well resolved from the adjacent photopeak at 511 keV. The resulting values for the events under the 478 keV photopeak were as follows: 4.17±0.90 cps and 4.84±0.86 cps for the 0 g measurements; 11.91±1.31 cps and 11.55±0.92 cps for the measurements at 0.5 g; 18.68±1.07 cps and 19.33±1.23 cps for the measurements at 1 g. After averaging each set of measurement and subtracting the 0 g value from the others, the final values were determined as 7.22 cps for the 0.5 g measurement and 15.5 cps for the 1 g measurement.

3.2. Imaging results

The reconstructed images were represented as 64 × 64 matrices, with pixel size of 0.78 mm. In Fig. 2, the images corresponding to the 1 g borated vial positioned at the center of the collimator hole (2b) and then shifted of 1 cm to the right (2a) and to the left (2c), respectively, are visible. The calculated mean Full Width at Half Maximum (FWHM) of the reconstructed positions for the three points was approximately 8 mm.

4. Discussion

The proposed detection unit has successfully demonstrated its capability to identify the BNCT photopeak. It has to be noted that the ^{10}B quantities used in the vials were considerably higher than the clinical range of 20–50 μg [2]. However, the neutron flux employed is considerably lower than the clinical standard of 10^9 n/cm^2/s, as is the measurement time, which is typically on the order of 30 min. Furthermore, the final SPECT system will be envisioned with multiple detectors. From
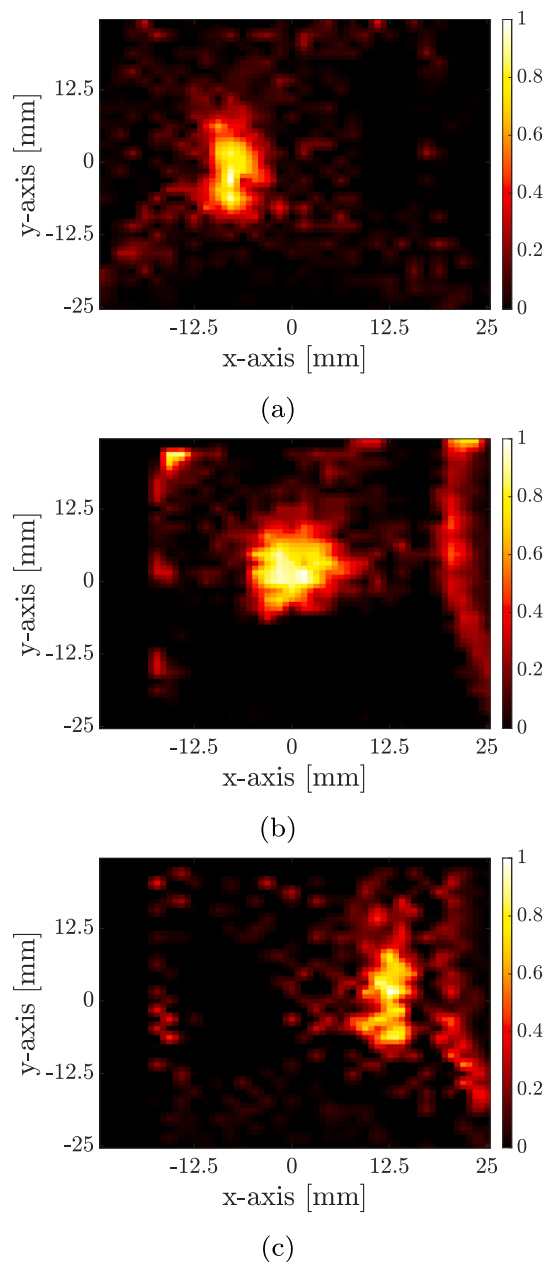

Fig. 2. Projection images of the vial loaded with 1 g of boron powder on the detector. (a) The vial is shifted 1 cm to the right from the center position; (b) the vial is aligned with the center of the collimator hole; (c) the vial is shifted 1 cm to the left. The colorbars indicate the pixels' intensities.

Fig. 1 it can be seen that the photopeaks at 558 keV and 651 keV due to cadmium neutron captures, while not affecting the 478 keV photopeak, raise concerns about detector counting rate and overall background radiation. To address this, lead foils can be extensively placed on the detector, not just on the lateral sides as done during the experiment due to limited availability, and their thickness can be increased. Focusing on the BNCT photopeak, the results highlight a significant reduction in background counts compared to our previous work [15], showing improved sensitivity of the presented detection module. The linear response is verified since counts at 478 keV double when the boron quantity doubles.

Regarding the imaging capability with the dedicated ANN, the system successfully tracked 1 cm shifts of the borated vial (Fig. 2). The flipping effect is attributed to the properties of the pinhole collimator which creates inverted projection images on the detector. The values of

the FWHM of the reconstructed positions are consistent with the spatial resolution of 8 mm imposed by the collimator and meet the 1 cm requirement.

In the context of detectors for BNCT applications, the proposed LaBr$_3$-based detector achieves a good balance between detection efficiency and energy resolution. Although its energy resolution may be lower than alternatives like CdTe and CZT detectors [8], our achieved results demonstrate its capability to effectively resolve the 478 keV photopeak from the adjacent photopeak at 511 keV. Several scintillator-based SPECT systems have been proposed and tested [6,7,21], including a tomographic test conducted with a LaBr$_3$-based pixelated detector [22]. Our study presents the first results obtained using a monolithic crystal combined with a pinhole collimator. Despite the increased challenge in reconstructing positions within a monolithic crystal compared to a pixelated one, our findings demonstrate remarkable spatial resolution results. With the spectroscopic and imaging outcomes obtained, we affirm the suitability of the proposed detector for the development of a BNCT-SPECT system.

CRediT authorship contribution statement

Anita Caracciolo: Conceptualization, Methodology, Validation, Formal Analysis, Investigation, Data Curation, Visualization, Writing – original draft. **Tommaso Ferri:** Methodology, Software, Formal Analysis, Data Curation, Visualization, Writing – review & editing. **Giacomo Borghi:** Funding acquisition, Supervision, Writing – review & editing. **Marco Carminati:** Funding acquisition, Supervision, Writing – review & editing. **Nicoletta Protti:** Resources, Writing – review & editing. **Saverio Altieri:** Resources, Writing – review & editing. **Carlo Fiorini:** Conceptualization, Project administration, Funding acquisition, Supervision, Writing – review & editing.

Declaration of Competing Interest

The authors declare that they have no known competing financial interests or personal relationships that could have appeared to influence the work reported in this paper.

Acknowledgements

References

[1] Sauerwein WAG, Wittig A, Moss R, Nakagawa Y, Sauerwein WAG, Wittig A, et al. Neutron capture therapy – principles and applications. 1st ed. Berlin Heidelberg (Germany): Springer-Verlag, Berlin Heidelberg 2012; 2012.
[2] Barth RF, Mi P, Yang W. Boron delivery agents for neutron capture therapy of cancer. Cancer Commun 2018;38:35. https://doi.org/10.1186/s40880-018-0299-7.
[3] Laakso J, Kulvik M, Ruokonen I, Vähätalo J, Zilliacus R, Färkkilä M, et al. Atomic emission method for total boron in blood during neutron-capture therapy. Clin Chem 2001;47:1796–803. https://doi.org/10.1093/clinchem/47.10.1796.
[4] Ishiwata K. 4-Borono-2-18F-fluoro-l-phenylalanine PET for boron neutron capture therapy-oriented diagnosis: overview of a quarter century of research. Ann Nucl Med 2019;33:223–36. https://doi.org/10.1007/s12149-019-01347-8.
[5] Kobayashi T, Sakurai Y, Ishikawa M. A noninvasive dose estimation system for clinical BNCT based on PG-SPECT—conceptual study and fundamental experiments using HPGe and CdTe semiconductor detectors. Med Phys 2000;27:2124–32. https://doi.org/10.1118/1.1288243.
[6] Kim M, Hong BH, Cho I, Park C, Min S-H, Hwang WT, et al. Design of a scintillator-based prompt gamma camera for boron-neutron capture therapy: comparison of SrI2 and GAGG using Monte-Carlo simulation. Nucl Eng Technol 2021;53:626–36. https://doi.org/10.1016/j.net.2020.07.010.
[7] Murata I, Kusaka S, Minami K, Saraue N, Tamaki S, Kato I, et al. Design of SPECT for BNCT to measure local boron dose with GAGG scintillator. Appl Radiat Isot 2022;181:110056. https://doi.org/10.1016/j.apradiso.2021.110056.
[8] Hales B, Katabuchi T, Igashira M, Terada K, Hayashizaki N, Kobayashi T. Predicted performance of a PG-SPECT system using CZT primary detectors and secondary Compton-suppression anti-coincidence detectors under near-clinical settings for boron neutron capture therapy. Nucl Instrum Methods Phys Res A 2017;875:51–6. https://doi.org/10.1016/j.nima.2017.09.009.
[9] Ishikawa M, Kobayashi T, Sakurai Y, Kanda K. Optimization technique for a prompt gamma-ray SPECT collimator system. J Radiat Res 2001;42:387–400. https://doi.org/10.1269/jrr.42.387.
[10] Abbene L, Principato F, Buttacavoli A, Gerardi G, Bettelli M, Zappettini A, et al. Potentialities of high-resolution 3-D CZT drift strip detectors for prompt gamma-ray measurements in BNCT. Sensors 2022;22. https://doi.org/10.3390/s22041502.
[11] Gong C, Tang X, Shu D, Yu H, Geng C. Optimization of the Compton camera for measuring prompt gamma rays in boron neutron capture therapy. Appl Radiat Isot 2017;124:62–7. https://doi.org/10.1016/j.apradiso.2017.03.014.
[12] Sakai M, Tamaki S, Murata I, Parajul RK, Matsumura A, Kubo N, et al. Experimental study on Compton camera for boron neutron capture therapy applications. Sci Rep 2023;13:22883. https://doi.org/10.1038/s41598-023-49955-9.
[13] Gola A, Acerbi F, Capasso M, Marcante M, Mazzi A, Paternoster G, et al. NUV-sensitive silicon photomultiplier technologies developed at Fondazione Bruno Kessler. Sensors 2019;19. https://doi.org/10.3390/s19020308.
[14] Buonanno L, Vita DD, Carminati M, Fiorini C. GAMMA: A 16-channel spectroscopic ASIC for SiPMs readout with 84-dB dynamic range. IEEE Trans Nucl Sci 2021;68:2559–72. https://doi.org/10.1109/TNS.2021.3107333.
[15] Caracciolo A, Di Vita D, Buonanno L, Carminati M, Protti N, Altieri S, et al. Experimental validation of a spectroscopic gamma-ray detector based on a LaBr 3 scintillator towards real-time dose monitoring in BNCT. Nucl Instrum Methods Phys Res A 2022;1041:167409. https://doi.org/10.1016/j.nima.2022.167409.
[16] Caracciolo A, Buonanno L, Di Vita D, D'Adda I, Chacon A, Kielly M, et al. BeNEdiCTE (Boron Neutron Capture): a versatile gamma-ray detection module for boron neutron capture therapy. IEEE Trans Radiat Plasma Med Sci 2022;6:886–92. https://doi.org/10.1109/TRPMS.2022.3154232.
[17] Morozov A, Solovov V, Martins R, Neves F, Domingos V, Chepel V. ANTS2 package: simulation and experimental data processing for Anger camera type detectors. J Instrum 2016;11:P04022. https://doi.org/10.1088/1748-0221/11/04/P04022.
[18] Battistoni G, Bauer J, Boehlen TT, Cerutti F, Chin MPW, Dos Santos Augusto R, et al. The FLUKA code: an accurate simulation tool for particle therapy. Front Oncol 2016;6. https://doi.org/10.3389/fonc.2016.00116.
[19] Giuntini L, Castelli L, Massi M, Fedi M, Czelusniak C, Gelli N, et al. Detectors and cultural heritage: the INFN-CHNet experience. Appl Sci 2021;11. https://doi.org/10.3390/app11083462.
[20] Knoll GF. Radiation detection and measurement. John Wiley & Sons; 2010.
[21] Okazaki K, Tanaka H, Takata T, Kawabata S, Akabori K, Sakurai Y. Evaluation of the energy resolution of a prompt gamma-ray imaging detector using LaBr 3(Ce) scintillator and 8 8 array MPPC for an animal study of BNCT. Appl Radiat Isot 2020;163:109214. https://doi.org/10.1016/j.apradiso.2020.109214.
[22] Minsky DM, Valda AA, Kreiner AJ, Green S, Wojnecki C, Ghani Z. First tomographic image of neutron capture rate in a BNCT facility. Special Issue: 14th International Conference on Neutron Capture Therapy 2011;69:1858–61. doi:10.1016/j.apradiso.2011.01.030.